



**HAL**  
open science

## Ultrasound-stimulated Brownian ratchet enhances diffusion of molecules retained in hydrogels

Faezeh Gerayeli, Nawel Khalef, Aziz Bakri, Philippe Benech, Donald Martin

### ► To cite this version:

Faezeh Gerayeli, Nawel Khalef, Aziz Bakri, Philippe Benech, Donald Martin. Ultrasound-stimulated Brownian ratchet enhances diffusion of molecules retained in hydrogels. *Nanomedicine: Nanotechnology, Biology and Medicine*, 2021, 31, pp.102308. 10.1016/j.nano.2020.102308 . hal-02987851

**HAL Id: hal-02987851**

**<https://hal.science/hal-02987851>**

Submitted on 7 Nov 2022

**HAL** is a multi-disciplinary open access archive for the deposit and dissemination of scientific research documents, whether they are published or not. The documents may come from teaching and research institutions in France or abroad, or from public or private research centers.

L'archive ouverte pluridisciplinaire **HAL**, est destinée au dépôt et à la diffusion de documents scientifiques de niveau recherche, publiés ou non, émanant des établissements d'enseignement et de recherche français ou étrangers, des laboratoires publics ou privés.



Distributed under a Creative Commons Attribution - NonCommercial 4.0 International License

1 **Ultrasound-stimulated Brownian ratchet enhances diffusion of molecules retained in**  
2 **hydrogels**

3

4 Faezeh Gerayeli <sup>a</sup>, Nawel Khalef <sup>b</sup>, Aziz Bakri <sup>b</sup>, Philippe Benech <sup>c</sup>, Donald K. Martin <sup>a\*</sup>

5

6 Affiliations:

7 *(a) Univ. Grenoble Alpes, CNRS, Grenoble INP, TIMC-IMAG / SyNaBi (UMR 5525),*  
8 *38000 Grenoble, France.*

9 *(b) Univ. Grenoble Alpes, CNRS, Grenoble INP, TIMC-IMAG / Pharmaceutical*  
10 *Engineering (UMR 5525), 38000 Grenoble, France.*

11 *(c) Univ. Grenoble Alpes, Grenoble INP, G2ELab, 38000 Grenoble, France.*

12

13 \*Corresponding author:

14 Donald Martin, don.martin@univ-grenoble-alpes.fr (tel : +33 4 56 52 00 95),

15 Université Grenoble Alpes, TIMC-IMAG (UMR 5525), Pavillon Taillefer, Domaine de la

16 Merci, 38706 La Tronche, France

17

18

19 Word Counts:

20 Abstract: 148

21 Complete manuscript: 5,255

22

23 Number of figures: 5

24 Number of tables: 1

25

26 **Abstract**

27 We demonstrate that low-frequency ultrasonic stimulation applied directly to a hydrogel, at  
28 energy levels below the cavitation threshold, can control the release of a therapeutic molecule.  
29 The hydrogel that contained the molecules was enclosed within a hollow acoustic horn. The  
30 harmonic modes in the acoustic horn combined with the physical gel structure to induce a  
31 flashing ratchet that released all of the retained molecules in less than 90 seconds at an  
32 intensity of  $1.5 \text{ W cm}^{-2}$  (applied energy of  $135 \text{ J cm}^{-2}$ , ultrasound center frequency of  
33  $27.9 \pm 1.5 \text{ kHz}$ ). In contrast, ultrasound is used currently as a remote stimulus for drug-delivery  
34 systems, at energy levels above the cavitation threshold. The low-energy flashing ratchet  
35 approach that we describe is applicable to drive the diffusion of molecules in a range of gels  
36 that are ubiquitous in biomedical systems, including for example in drug delivery, molecule  
37 identification and separation systems.

38

39 **Keywords:** Hydrogel structure, directed diffusion, flashing ratchet, ultrasound, harmonic  
40 modes, acoustic horn

41

## 42 **Background**

43 The system we describe provides a novel approach to the use of a low-frequency ultrasound  
44 transducer to stimulate diffusion in hydrogels. A custom-made hollow acoustic horn was  
45 firmly attached to a low-frequency ultrasound transducer. The hollow acoustic horn enclosed  
46 a hydrogel that contacted all sides of the acoustic horn except for one surface of the hydrogel  
47 that allowed for release of the molecules retained in the hydrogel. The advantage of this  
48 configuration is that low-frequency ultrasound could be applied at a sufficiently low intensity  
49 so as not to induce cavitation in the hydrogel. The novelty of this hydrogel delivery system is  
50 that the combination of the physical hydrogel structure and the non-linear harmonic effects in  
51 the hollow acoustic horn created a Brownian flashing ratchet that was effective in directing  
52 the movement of molecules rapidly to the exit surface of the hydrogel. The acoustic horn was  
53 stimulated with externally applied ultrasound with a center frequency of  $27.93 \pm 1.47$  kHz and  
54 at intensities  $0.4 \text{ W cm}^{-2}$  (minimum) and  $1.5 \text{ W cm}^{-2}$  (maximum), both of which were below  
55 the cavitation threshold.

56

57 A low-frequency acoustic horn is a common device but with a complex operating mode. The  
58 most common usage of such horns is to generate 20–30 kHz continuous-wave fields into  
59 water or an aqueous solution that has undergone no special treatment (such as degassing or  
60 deionizing) under atmospheric pressure [1]. In those previous studies where the low-  
61 frequency ultrasound horn was positioned remotely at some distance from the polymer or the  
62 skin (for sonophoresis), the power required was above the cavitation threshold. For example,  
63 for sonophoresis the maximum enhanced transport occurred at power levels of about  $14 \text{ W}$   
64  $\text{cm}^{-2}$  (for 20 kHz) and  $17 \text{ W cm}^{-2}$  (for 40 kHz), which induce cavitation [2]. Indeed,  
65 intensities of low-frequency ultrasound (23 kHz) above such cavitation thresholds have been  
66 reported to degrade polyvinyl alcohol (PVA) by breakage of chemical bonds within the

67 polymer due to shear forces generated by rapid motion of the solvent following cavitation  
68 collapse [3].

69

## 70 **Methods**

### 71 *Low-frequency Ultrasound System*

72 The source of this low-frequency ultrasound was a dental ultrasonic scaler (Guilin  
73 Woodpecker, UDS-K) that the manufacturer specified as providing ultrasound at the  
74 frequency of  $28 \pm 3$  kHz. The dental scaler had a screw-thread on the transducer to provide a  
75 stable means to connect dental endpiece tools to the transducer. This screw-thread was used to  
76 firmly connect our custom-made hollow acoustic horns. In order to measure the effect of  
77 ultrasound on drug release in real-time from the custom-made hollow acoustic horns an  
78 experimental set-up was designed that comprised a custom-made ultrasonic exposure  
79 chamber, a UV-Vis spectrophotometer and a peristaltic pump. Thin plastic tubing is used to  
80 connect different parts of the set-up and to form a fluid-flow circuit (Figure 1).

81

### 82 *Chemicals*

83 Low melting temperature agarose (NuSieve GTG Agarose) was purchased from Lonza  
84 Walkersville, Inc. and used as received throughout the research. Polyvinyl alcohol, PVA,  
85 (MW=125000) was purchased from SDFine Chem Ltd (Mumbai, India). Dimethyl sulfoxide  
86 (DMSO) was purchased from Sigma. Chitosan (medium MW, code:448877) and acetic acid  
87 were purchased from Sigma.

88

### 89 *Hydrogel Preparation*

90 Three types of hydrogel were prepared for these experiments; agarose, PVA cross-linked with  
91 DMSO, and a chitosan/agarose blend. These hydrogels are representative of physical hydrogel

92 (agarose), blended polymer (chitosan/agarose), and a chemically crosslinked hydrogel (PVA).  
93 For the agarose hydrogel, a 2% w/v agarose solution was prepared in distilled water. For the  
94 chitosan/agarose blend hydrogel, a 2% w/v chitosan solution was prepared in a 1.0% w/v  
95 aqueous acetic acid since this acidic condition ( $\text{pH} < 6.5$ ) assisted the solubility of the  
96 chitosan due to the electrostatic effect among the protonated amine groups along the polymer  
97 chains. First, the acetic acid solution was prepared at  $60^\circ\text{C}$ , then the beaker was removed from  
98 the heater and chitosan was added slowly to the acetic acid while stirring to achieve a final  
99 concentration of 2% w/v chitosan in the solution. Since chitosan alone does not form a stable  
100 hydrogel, a blended hydrogel mixture of 25% v/v agarose and 75% v/v chitosan was prepared  
101 by adding slowly a 2% w/v agarose solution to the 2% w/v chitosan solution while stirring at  
102 room temperature to obtain a homogenous mixture that became progressively more viscous.  
103 Under these conditions the hydrogels blended to form a homogenous phase with extended  
104 chitosan chains within the agarose matrix [4]. The blended hydrogel mixture retained  
105 transparency, which suggested the uniform distribution of chitosan in the agarose matrix  
106 without noticeable phase separation due to the hydrogen bonds between the chitosan amino  
107 groups and agarose hydroxyl groups [5]. For the PVA cross-linked hydrogel, a mixture  
108 DMSO (40%) and water (60%) was used as the solvent. The solvent was heated to  $90^\circ\text{C}$  in a  
109 water bath while being stirred. PVA powder was added to the hot solvent and was stirred until  
110 obtain a 15% w/v PVA homogenous solution.

111

112 Those three different polymer solutions were poured into the hollow acoustic horns shown in  
113 Figure 1 and then left at the ambient temperature to obtain hydrogels to be used for further  
114 experiments.

115

116 *Measurement of the Ultrasound Intensity*

117 The Guilin Woodpecker ultrasonic scaler included a variable power dial so that the intensity  
118 of ultrasonic could be changed. The intensity of ultrasound at each power setting was  
119 measured using a calorimetric method that is based on the change of temperature in water  
120 exposed to the sonicator [6, 7]. A plastic beaker, thermally insulated with expanded  
121 polystyrene, was filled with 40 mL water. The ultrasound horn, corresponding to the position  
122 of the drug carrier, was immersed into water. The ultrasound device was activated for 2 min at  
123 each of the positions indicated on the sonicator power dial. The rate of increase in water  
124 temperature was measured using a type N thermocouple (TC S.A., France) with a sensitivity  
125 of  $39 \mu\text{V C}^{-1}$  at  $900^\circ\text{C}$ . The equation below was then used to calculate the intensity:

126

$$127 \quad I = \frac{M_{\text{Water}} C_{p.\text{Water}}}{A} \frac{\Delta T}{\Delta t} \quad (1)$$

128

129 where  $I$  is the ultrasound intensity ( $\text{W cm}^{-2}$ ),  $M_{\text{water}}$  is the mass of water exposed (g),  $C_{p.\text{water}}$  is  
130 the specific heat of water ( $4.18 \text{ J g}^{-1} \text{ C}^{-1}$ ),  $A$  is the effective area of the transducer and  $\Delta T/\Delta t$  is  
131 the rate of temperature change of the water. In using this equation, we assume that the  
132 temperature change of water is due to incident acoustic power, and the acoustic power is  
133 completely converted into heat.

134

### 135 *Measurement of the Actual Frequency and Harmonics in the Acoustic Horns*

136 Although the manufacturer specified the frequency generated by the Guilin Woodpecker  
137 ultrasonic scaler to be in the range of  $28 \pm 3 \text{ kHz}$ , the characteristics of the ultrasound  
138 generated in each acoustic horn required verification. To measure the actual frequency inside  
139 the different acoustic horns polyvinylidene fluoride (PVDF) was used as a sensor for the  
140 ultrasound since it is a piezoelectric polymer with high sensitivity. PVDF was placed in direct  
141 contact with each transducer horn at the face  $d_1$  (Figure 1). The PVDF was connected to an

142 oscilloscope (Tektronix) to detect and record the frequency of the generated ultrasound. These  
143 characteristics of the actual ultrasound frequencies and harmonics are important for the  
144 interpretation of the release of compounds from the gels that were enclosed within each  
145 acoustic horn.

146

#### 147 *Measurement of vibration in the acoustic horn*

148 We assumed that in our drug delivery device the energy imparted by the longitudinal  
149 ultrasonic waves and harmonics were solely responsible for the release of the active agent  
150 from the polymer matrix. A possible alternative was that the ultrasound simply caused the  
151 lateral displacement of the horn due to the vibration caused by the ultrasound transducer, and  
152 this vibration was simply the stimulus for the drug release from the hydrogel. To test this  
153 possibility the vibration of the transducer with and without the horn was measured using a  
154 vibrometer (Keyence, LK-G3000) when ultrasound waves were generated by the Guilin  
155 Woodpecker ultrasonic scaler. The vibrometer provided a very sensitive measurement of the  
156 displacement at an accuracy of 0.05  $\mu\text{m}$  and a linearity of 0.03% F.S.

157

## 158 **Results**

### 159 *The measured ultrasound frequencies and harmonics in the acoustic horns*

160 The shape and size of the acoustic horn were chosen so as to optimize the constructive  
161 harmonics generated by the ultrasound, which provided the power to drive the movement of  
162 the molecules retained in the hydrogel to be released at the exit-surface of the hydrogel  
163 (Figure 1). The characteristics of the ultrasound harmonics were determined for each of the  
164 acoustic horns from measurements performed with the release-surface aspect  $d_1$  of the  
165 acoustic horn placed firmly in-contact with a piezoelectric polymer (polyvinylidene fluoride,  
166 PVDF) that was connected to an oscilloscope. Measurements were carried out on the three

167 sizes of horns, with or without hydrogel inside the horn. Figure 2 shows the spectrum of  
168 harmonics generated in the acoustic horns. The spectra recorded were the same whether or not  
169 the hydrogel was enclosed within the horn. Moreover, the center frequency of  
170  $27.93 \pm 1.47$  kHz was the same for all sizes of the horns. However, amongst the horns of  
171 different sizes there are differences in the harmonics of the center frequency. These harmonics  
172 are due to the nonlinear behavior of the piezoelectric transducer [8–10]. The amplitude of  
173 harmonics depends on the excitation intensity delivered to the transducer and on the  
174 configuration of the horn, particularly since the type of horn provides a mechanical load for  
175 the transducer. The small horn produced the strongest harmonics and the highest amplitude of  
176 the fundamental. For the small horn, it is notable that at the higher intensity there is a  
177 doubling of the harmonics (Figure 2, E and F). The increase in amplitude of harmonics may  
178 be due not only to the excitation intensity but also to the constructive interference of the  
179 ultrasound waves within the horn due to reverberation and reflection from the walls, which  
180 would indicate the presence of several modes of ultrasound generated in the horn. These types  
181 of reverberations and reflections, in the absence of cavitation, have also been reported for  
182 cylindrical sonochemical reactors [11]. Increasing the horn size from medium to large reduced  
183 the prominent harmonics, most likely due to destructive interference within the horn, since  
184 there are fewer harmonics and no change with intensity. This most likely would minimize the  
185 amount of energy imparted to the hydrogel drug carrier, with the practical effect to reduce the  
186 stimulus for controlling diffusion of molecules retained in a hydrogel carrier. We can conclude  
187 that with the small horn there is an optimization of the ultrasound harmonics, which probably  
188 increased the modes and energy delivery within the small horn. Thus, the small horn could be  
189 expected to provide a better stimulus for the motion of a molecule retained in the hydrogel  
190 and would most likely increase the efficiency of directed motion of the retained molecule in  
191 the hydrogel. Moreover, any differences in the release rates of compounds from the horns

192 could be interpreted from the minimization of the harmonics by increasing the diameter of the  
193 acoustic horns, since the center frequency was the same for each horn and thus each horn  
194 received the same longitudinal acoustic energy.

195

#### 196 *The ultrasound intensity in the acoustic horns*

197 We used a calorimetric method to measure the intensity generated in the acoustic horns by the  
198 ultrasound transducer [6, 7]. The intensities in the large horn were between  $0.02 \text{ W cm}^{-2}$   
199 (minimum) and  $0.11 \text{ W cm}^{-2}$  (maximum), in the medium horn were between  $0.08 \text{ W cm}^{-2}$   
200 (minimum) and  $0.19 \text{ W cm}^{-2}$  (maximum), and in the small horn were between  $0.4 \text{ W cm}^{-2}$   
201 (minimum) and  $1.5 \text{ W cm}^{-2}$  (maximum). It is important to note that all of those measured  
202 intensity levels for all of the horns are below the threshold level to induce cavitation in water.

203

204 The higher intensities measured for the small horn were most likely due to the efficient  
205 generation of constructively interfering harmonics (Figure 2, E and F). For the small horn, the  
206 measured temperature was similar at the center and at the wall of the horn. This indicated that  
207 the intensity was evenly distributed across the area of the exit-surface of the small horn.

208 Moreover, that energy dissipated quickly after the exit-surface of the small horn since the  
209 measured temperature was lower at a distance of 1.5 mm from the exit-surface.

210

#### 211 *Does the ultrasound simply vibrate the acoustic horn?*

212 We used a sensitive vibrometer to determine if the acoustic horns were simply being vibrated  
213 by the ultrasound transducer. The vibrometer detected no displacement of any of the horns,  
214 which indicated that vibration of each horn was smaller than the level of the sensitivity of the  
215 instrument ( $0.05 \mu\text{m}$ ). Hence it was unlikely that the release phenomena were due simply to  
216 mechanical vibration of the horns that may have produced material stretching the gels.

217

218 *Do the enhanced harmonics of the small horn increase the rate of release from a hydrogel?*

219 Our first experiments were aimed to confirm the advantages of the small horn, compared to  
220 other sized horns, to stimulate the diffusion of molecules within a hydrogel retained inside the  
221 hollow horn. These experiments were performed using 2% w/v agarose prepared in distilled  
222 water, since this is a physical gel with a non-complex structure. We used theophylline to  
223 investigate the efficiency of the ultrasound to stimulate the diffusion of molecules. A  
224 theophylline stock solution of 4.7 mg mL<sup>-1</sup> was prepared in deionized water by heating at  
225 30°C until obtaining a clear solution. To load drug in the agarose gel, fresh agarose solution  
226 was mixed with theophylline (30% v/v) and immediately vortexed for 15 seconds to obtain a  
227 homogeneous distribution of theophylline. This theophylline-loaded agarose solution was  
228 then injected into the ultrasound horn and allowed to gel at room temperature. The mass of  
229 retained theophylline was 2.37 mg for the large horn, 0.94 mg for the medium horn and 0.15  
230 mg for the small horn. Figure 3 shows the results of these optimization experiments. Release  
231 of theophylline from the agarose was measured, using the UV-Vis spectrometer, by an  
232 increase in the absorbance at 272 nm.

233

234 For the small horn, all the theophylline was released in less than 90 seconds when the  
235 intensity was 1.5 W cm<sup>-2</sup>. For the lowest intensity of 0.4 W cm<sup>-2</sup> the theophylline was  
236 completely released from the small horn after about 3 minutes (Figure 3). The corresponding  
237 energy dose for the small horn was between 72 J cm<sup>-2</sup> to 135 J cm<sup>-2</sup>. This is a much lower  
238 than the reported threshold energy dose of 222 J cm<sup>-2</sup> for pig skin in vitro that is required for  
239 cavitation effects to stimulate the sonophoretic enhancement of transport at 20 kHz [12].  
240 Indeed, Mitagotri et al [13] reported that the minimum ultrasound intensity required for the

241 onset of cavitation, referred to as the cavitation threshold, increases rapidly with ultrasound  
242 frequency up to a maximum of 2.5 MHz.

243

244 The rapid and efficient release with the low intensity from the small horn was most likely due  
245 to the enhanced harmonics that have led to constructive interference of the ultrasound waves.  
246 For the two other horn sizes (medium and large) the time needed for complete drug release  
247 was more than 24 hours, most likely due to the destructive interference of the harmonics of  
248 the ultrasound stimulation. Those differences in release rates between the sizes of the acoustic  
249 horn also highlight that the release could not have resulted simply from the longitudinal  
250 transmission of acoustic energy, since the center frequency of the ultrasound was the same for  
251 each of the horns. It is also unlikely that the differences between release rates was due to  
252 vibrations of the horns, since the vibrometer did not detect a vibration of any of the horns (any  
253 vibration was less than the sensitivity of the instrument, 0.05  $\mu\text{m}$ ).

254

255 Thus, the small acoustic horn was selected for the following experiments in which we  
256 measured the release of theophylline from the chitosan/agarose blend, agarose and PVA  
257 hydrogels. Figure 4 summarizes the results from measuring 5 replicates for each hydrogel that  
258 show the release of theophylline from each of the hydrogels. The slower release from the  
259 PVA, and indeed the difference between the chitosan/agarose and agarose, were most likely  
260 due to the physico-chemical structure of each hydrogel. Those details of the influence of the  
261 chemistry of the hydrogel structure are being characterized in other parallel studies in our  
262 laboratory. Nonetheless, for all 3 hydrogel samples that were stimulated with the ultrasound,  
263 increasing the ultrasound intensity from 0.4  $\text{W cm}^{-2}$  to 1.5  $\text{W cm}^{-2}$  has nearly doubled the rate  
264 of release from all three hydrogel carriers. In considering the data of Figure 4, it is important  
265 to compare the diffusion of theophylline without any applied ultrasound stimulus to the small

266 horn. During a period of 5 minutes with no ultrasound stimulation to the small horn only  
 267 about 15% of the theophylline diffused from the agarose, only about 5% diffused from the  
 268 PVA and only about 20% diffused from the chitosan/agarose (Figure 5). The ultrasound-  
 269 stimulated release rate of theophylline from different hydrogels was calculated from the first  
 270 linear part of the release curve (Figure 4) and presented in Table 1. These tabulated data  
 271 emphasize the role of ultrasound in controlling the drug release, but with an influence from the  
 272 structure of the different polymeric networks, particularly when compared to the slow passive  
 273 diffusional release measured without external stimulation.

274

275 **Table 1:** Rate of release from the chitosan/agarose blend, agarose, and PVA hydrogels at  
 276 different ultrasound intensities ( $0.4 \text{ W cm}^{-2}$ ,  $1.5 \text{ W cm}^{-2}$ ). The rate of release is calculated  
 277 from the initial linear part of the release curves shown in Figure 4.

278

	<b>Release Rate (<math>\text{s}^{-1}</math>)</b>	
	at $0.4 \text{ W cm}^{-2}$	at $1.5 \text{ W cm}^{-2}$
<b>Agarose</b>	0.717	1.205
<b>PVA</b>	0.114	0.283
<b>Chitosan/agarose blend</b>	1.462	3.291

279

280

281 *Does the ultrasound simply induce cavitation or gel breakdown to enhance diffusion?*

282 During control experiments where theophylline was not loaded into the hydrogels there was  
 283 no absorbance at 272 nm detected in the release media after a 2-hour continuous period of  
 284 ultrasound stimulation. These control experiments support the observations that all three  
 285 hydrogels are stable and do not release any breakdown products at the absorbance peak of  
 286 theophylline. Further, these control absorbance measurements during 2 hours of continuous  
 287 ultrasound stimulation suggests that the shorter periods of ultrasound required to induce the  
 288 ratchet effect stimulation would not degrade the gels.

289

290 It is important to note that all of the intensity levels to induce the ratchet effect are below the  
291 threshold level to induce cavitation in water. Moreover, the intensities in the acoustic horns  
292 generated by the ultrasound were much less than the threshold reported to cause breakdown of  
293 PVA due to cavitation collapse [3]. It is possible that the ultrasound energy may have  
294 generated sufficient heat that may have caused the hydrogels to melt during the period  
295 required for release of the theophylline, thereby contributing to the enhanced diffusion.  
296 Increasing the intensity increases the energy of the waves and the energy transferred to the  
297 hydrogel. This could augment the amount of the heat produced by the absorption of  
298 ultrasound waves when applying a higher intensity. The same effect could be expected for the  
299 exposure time. If the theophylline molecules in the hydrogel absorb an amount of energy for a  
300 longer duration, there is potentially an increase in the total amount of the energy absorbed and  
301 consequently an increase in gel temperature.

302

303 However, the maximum energy dose delivered to the gels was  $135 \text{ J cm}^{-2}$  and such an energy  
304 dose could be expected to increase the temperature of the hydrogels by around  $10 \text{ C}^\circ$  [14].  
305 The measurements were made at room temperature,  $20 \text{ }^\circ\text{C}$ . We found previously, using  
306 differential scanning calorimetry, that the onset melting temperatures for these hydrogels  
307 ranged from  $49^\circ\text{C}$  (chitosan/agarose blend), to  $50^\circ\text{C}$  (alginate), to around  $190^\circ\text{C}$  (PVA) [15].  
308 At temperatures less than the onset melting temperature the elastic modulus and porous  
309 structure of the gel remain stable [16]. Thus, it is unlikely that ultrasound energy induced an  
310 increase in temperature that caused the structure of the hydrogels to breakdown. We used a  
311 simple observation to observe melting-induced changes of the hydrogels when the time of  
312 exposure and the ultrasound intensity were changed. For that observation, a thin metal wire  
313 was inserted into the hydrogel inside the horn and removed after a few seconds. If the  
314 hydrogel was melted, a thin viscous layer of hydrogel sol could be observed coating the

315 surface of the wire. Our observations using the small wire were that the gels showed signs of  
316 melting after around 280 seconds (chitosan/agarose) to 35 minutes (PVA). These periods were  
317 much longer than the time required for complete release of theophylline from the acoustic  
318 horns. Altogether, it is unlikely that any induced breakdown of the hydrogels contributed to  
319 the enhanced diffusion that was stimulated by ultrasound.

320

## 321 **Discussion**

322 The measurements carried out in this study indicate that low-frequency ultrasound, applied at  
323 intensities less than the cavitation threshold to a hydrogel contained within an appropriately  
324 dimensioned acoustic horn, directly enhances the diffusion of theophylline in the hydrogel.  
325 The mechanism of this action appears to be due to the constructive interference of the  
326 different harmonic modes of the fundamental of the ultrasound. Our experimental evidence to  
327 support this conclusion are that (i) the release rates from the hydrogel increased with  
328 reduction of diameter of the acoustic horn, (ii) the harmonics were enhanced with reduction of  
329 diameter of the acoustic horn, (iii) the centre frequency was the same for all acoustic horns of  
330 different diameter, and (iv) none of the acoustic horns were measurably vibrated by the  
331 ultrasound transducer (or less than the sensitivity of the measurement vibrometer, 0.05  $\mu\text{m}$ ).

332

333 To explain the mechanism of this enhanced diffusion of theophylline molecules, the hydrogel  
334 polymeric matrix can be considered as a mesh with pores that are relatively larger in size than  
335 the theophylline molecules. It is also important to consider the hydrogels have some amount  
336 of crystalline structure and a degree of viscoelasticity, with the theophylline molecules being  
337 homogeneously dispersed within the hydrogel matrix. The diffusion behavior of theophylline  
338 could be expected to be determined by the characteristic size of the theophylline molecules  
339 and the correlation length of the polymer network [17]. In the absence of the externally-

340 applied ultrasound, the diffusion of theophylline as the solute in the hydrogels could be  
341 explained in one of 4 main theoretical frameworks. These frameworks include the  
342 hydrodynamic mode (friction between the solute and the surrounding hydrogel matrix), the  
343 free-volume mode (transport of the solute via the dynamic empty spaces between molecules),  
344 the obstruction mode (polymer matrix functions as a barrier for the diffusion of solute), or a  
345 multiscale diffusion model (MSDM) that combines the hydrodynamic, free-volume and  
346 obstruction modes [18]. For all such considerations of the diffusion in hydrogels, the average  
347 mesh size of the polymeric matrix (the correlation length) compared to the hydrodynamic  
348 radius of the solute is an important parameter. For the hydrogels used in this report, the  
349 correlation length for the agarose and chitosan/agarose has been reported to be on the order of  
350 60 nm [19] to 200 nm [20]. For the PVA, the correlation length has been reported to be  
351 between 3.6 nm to 25 nm [21]. Theophylline has a molecular weight of 180 and an  
352 hydrodynamic radius of 0.35 nm [22]. The free volume of the hydrogel system was estimated  
353 to be on the order of 0.3 nm based on the the work of Axpe et al [18].

354

355 Without the application of ultrasound the release of theophylline in these hydrogels will be  
356 predominately explained by the free-volume mode of diffusion. Without ultrasound, the  
357 diffusion of theophylline would be quite slow, with reports of up to 180 minutes for the  
358 complete release of theophylline from an agarose hydrogel [23], and on the order of 225  
359 minutes from a PVA hydrogel [24]. Our results reported here agree with those previous  
360 measurements of slow release, since during a period of 5 minutes with no ultrasound  
361 stimulation to the small horn only about 15% of the theophylline diffused from the agarose,  
362 only about 5% diffused from the PVA, and only about 20% diffused from the chitosan. In  
363 contrast, here we report that the application of ultrasound to the hydrogels dramatically  
364 increased the rates of release of the theophylline from the hydrogels. An intensity of

365 ultrasound below the cavitation threshold was able to release 100% of the theophylline from  
366 the chitosan/agarose blended hydrogel in 90 seconds, and from the agarose hydrogel in 180  
367 seconds. Only 50% of the theophylline was released from the PVA hydrogel after 480  
368 seconds, most likely related to the smaller correlation length of the PVA hydrogel. Note that  
369 the hydrogels used for these experiments included hydrogels that were formed physically as  
370 well as one that was chemically cross-linked.

371

372 The rapid and controlled movement of molecules in the hydrogels can be explained by  
373 directed Brownian motion that results from the interplay between the ultrasound harmonics  
374 and the polymeric hydrogel structure in an analogous way to a flashing ratchet. The  
375 theophylline molecules can be considered as over-damped particles [25]. In all sizes of the  
376 horns (small, medium, large) there are the same continuous low-frequency compressive  
377 longitudinal ultrasound waves acting on the hydrogels. That low-frequency ultrasound,  
378 applied at the low intensities used here, would impart some momentum to the theophylline  
379 molecules that would then induce small motions. The combination of the hydrogel  
380 concentration (to alter the polymeric backbone structure and the viscoelasticity of the gel), the  
381 mass of the molecule, the power and the frequency of the ultrasound all combine to limit the  
382 range of such an imparted motion of the molecules, as has been shown for a system that  
383 contained gold nanoparticles [26]. Nonetheless, at a critical combination of low-frequency  
384 ultrasound at low power to induce a low acoustic pressure there will be sufficient time for the  
385 therapeutic agent molecules to be “pushed” through the hydrogel structure. The distance  
386 “pushed” will also be influenced by the viscoelastic forces in the hydrogel, which could serve  
387 to damp the ultrasound-imparted momentum and movement of the molecules. Without the  
388 generation of constructively interfering harmonics inside the medium and large acoustic  
389 horns, the theophylline molecules in the hydrogel are subjected simply to the longitudinal

390 ultrasound waves without any additional periodic stimulus to create an effective ratchet. Thus,  
391 the diffusion in the medium and large horns is not enhanced any controlled way more than  
392 from the compressive “pushes”.

393

394 However, the constructively interfering harmonics generated within the small horn provide  
395 the necessary external energy to drive the interplay of the theophylline molecules with the  
396 polymeric structure in order to create the flashing ratchet. In the hydrogel system contained  
397 within the small horn, the ultrasound harmonics provide a periodic signal that combines with  
398 the hydrogel structure to induce the rectification needed for the flashing ratchet. The  
399 importance of this combination is observed from Figure 4 where the enhanced diffusion-rate  
400 of the theophylline molecules is reduced in the PVA hydrogels. Compared to PVA, the  
401 agarose and chitosan/agarose have significantly greater water content and are physical  
402 hydrogels. Also, the correlation length of the PVA hydrogel is much smaller than that of  
403 either the agarose/chitosan blended hydrogel or the agarose hydrogel. In considering a  
404 framework within which to understand these enhanced diffusion phenomena, we can utilize  
405 the multiscale diffusion model (MDSM) that combines the major diffusional theories of free-  
406 volume, hydrodynamic and obstruction modes [18]. The advantages of the MDSM model are  
407 that it covers several correlation length scales and it incorporates both the free-volume and  
408 hydrodynamic modes of diffusion. For the chitosan/agarose blend and the agarose hydrogels  
409 the hydrodynamic radius of the theophylline is more than 100-fold less than the correlation  
410 length, the diffusion is dominated by the free-volume mode, and the flashing ratchet  
411 established by the constructive harmonics of the ultrasound provides the additional energy to  
412 drive the release of the theophylline at faster rates. Indeed, the correlation length of the  
413 chitosan/agarose blended hydrogel is larger (around 200 nm) than that for agarose (around 60  
414 nm), and the theophylline was released from the chitosan/agarose blended hydrogel at a faster

415 rate than for the agarose hydrogel. For the PVA hydrogel, the hydrodynamic radius of  
416 theophylline is only around 10-fold less than the correlation length. Although it is likely that  
417 the mode of diffusion continues to be dominated by free-volume, the reduced release rate  
418 from PVA compared to the agarose-based hydrogels is most likely due to an increased  
419 influence from hydrodynamic diffusion mode.

420

421 This study suggests that low-frequency ultrasonic stimulation, at energy levels below the  
422 cavitation threshold, can be used to control the release of a therapeutic molecule from  
423 different hydrogel carriers. Although ultrasound has been used previously as an external  
424 stimulus for enhancing mass-transport of drugs in drug delivery systems [27], most of the  
425 previous reports utilized an acoustic field generated by an ultrasonic horn immersed in a fluid  
426 chamber and located at some distance from a drug-containing polymer [28–30], or touching  
427 the skin to enhance transdermal transport via the mechanism of sonophoresis [2, 31]. For such  
428 sonophoresis-mediated transport it has been considered for some time that inertial cavitation  
429 is the mechanism that is responsible [13], due to the requirements to deliver high energy  
430 levels. Also, for example, therapeutic ultrasound (1 MHz) has been reported recently to  
431 trigger drug release from poly(lactide-co-glycolide) (PLGA) microchamber arrays that were  
432 implanted subcutaneously in a mouse [32].

433

434 In contrast to the previous ultrasound-generating devices used to enhance the transport of  
435 therapeutic molecules by the influence of inertial cavitation when remotely placed from the  
436 drug-containing polymer [27], the diffusion of molecules in our system was controlled using  
437 low-frequency ultrasound delivered directly to the hydrogel that was enclosed within a small-  
438 diameter hollow acoustic horn connected to the ultrasound transducer. Three types of porous  
439 hydrogels (PVA, chitosan/agaroseblend, and agarose) were tested separately as the hydrogel

440 matrix for theophylline, which was enclosed in the hollow acoustic horn. The transport of  
441 theophylline (representative molecule) to the exit-surface of the porous hydrogels at the  
442 opening of the acoustic horn was controlled by directed Brownian motion driven by the  
443 harmonics generated inside the acoustic horn. Moreover, this design required only a low  
444 intensity from the ultrasonic transducer, which was lower than the threshold for cavitation.  
445 Even with our direct-contact acoustic horn operating at its lowest intensity of  $0.4 \text{ W cm}^{-2}$ , the  
446 entire drug content of the hydrogel could be released in less than 3 minutes. In comparison,  
447 the previous systems with a remote ultrasound transducer that relied on cavitation needed  
448 several hours for complete release [27, 28, 30]. The use of hydrogels is ubiquitous for  
449 biomedical systems where the transport of molecules needs to be controlled, including for  
450 example drug delivery and molecule identification and separation systems. Indeed, since the  
451 the flashing ratchet we describe provides controllable energy inputs at levels less than those  
452 that neither induce breakdown of the gel structure nor induce cavitation, this flashing ratchet  
453 may be useful for further investigations of release in systems where there are important  
454 interactions between the solute and the gel. Such interactions could include hydrophobic  
455 effects, H-bonding, electrostatic, and van der Waals interactions [18].

456

457 The advantages of the approach described in this report are that (i) the directed diffusion of  
458 molecules was driven by a Brownian flashing ratchet due to the combination of the physical  
459 gel structure and the energy imparted by the ultrasound generated inside the hollow acoustic  
460 horn, (ii) a low level of acoustic energy was required to drive the transport in the hydrogel,  
461 and (iii) no cavitation was induced in the hydrogel, which minimized the potential for  
462 physico-chemical damage. This flashing ratchet approach is applicable to drive the diffusion  
463 of molecules in a range of gels that are ubiquitous in biomedical systems, including for  
464 example in drug delivery, molecule identification and separation systems.

465

## 466 **Acknowledgements**

467 The authors wish also to acknowledge financial assistance from the French Agence Nationale  
468 pour la Recherche (ANR-11-BSV5-009).

469

## 470 **Author contributions**

471 F.G. and D.K.M conceived the study. F.G. performed the experiments with N.W.  
472 (calorimetry), A.B. (diffusion), P.B. (ultrasonic characterization) and D.K.M (hydrogel). A.B.  
473 developed the set-up for ultrasound-stimulated diffusion measurements. F.G. analyzed the  
474 data with assistance from N.W., A.B., P.B. and D.K.M. The original draft was written by F.G.  
475 All authors contributed to the editing of revised drafts. D.K.M. supervised the research.

476

## 477 **Competing interests**

478 The authors declare no competing interests.

479

## 480 **References**

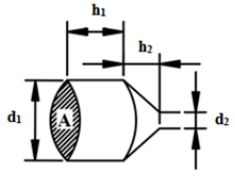
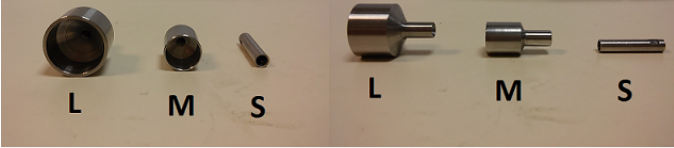
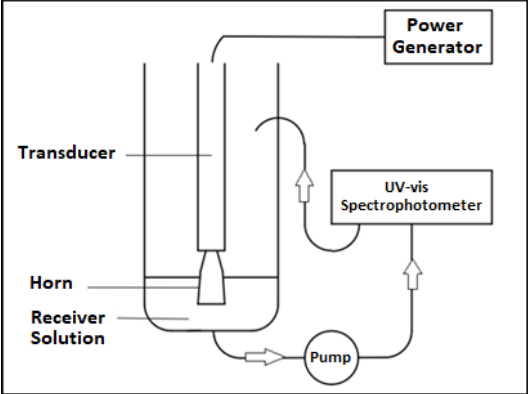
- 481 [1] Birkina PR, Offen DG, Vian CJB. Multiple observations of cavitation cluster dynamics  
482 close to an ultrasonic horn tip. *J Acoust Soc Amer* 2011;**130**:3379-3388.
- 483 [2] Terahara T, Mitragotri S, Kost J, Langer R. Dependence of low-frequency sonophoresis  
484 on ultrasound parameters; distance of the horn and intensity. *Intern J Pharmaceut*  
485 2002;**235**:35-42.
- 486 [3] Grönroos A, Pirkonen P, Heikkinen J, Ihalainen J, Mursunen H, Sekki H. Ultrasonic  
487 depolymerization of aqueous polyvinyl alcohol. *Ultrason Sonochem* 2001;**8**:259-264.
- 488 [4] Cao Z, Gilbert RJ, He W. Simple agarose-chitosan gel composite system for enhanced  
489 neuronal growth in three dimensions. *Biomacromolecules* 2009;**10**:2954–2959.

- 490 [5] Zamora-Mora V, Velasco D, Hernandez R, Mijangos C, Kumacheva E.  
491 Chitosan/agarose hydrogels: Cooperative properties and microfluidic preparation.  
492 *Carbohydr Polym* 2014;**111**:348–355.
- 493 [6] Mitragotri S, Blankschtein D, Langer R. Ultrasound-mediated transdermal protein  
494 delivery. *Science* 1995;**269**:850-853.
- 495 [7] Tezel A, Sens A, Tuchscherer J, Mitragotri S. Synergistic effect of low-frequency  
496 ultrasound and surfactants on skin permeability. *J Pharmaceut Sci* 2002;**91**:91-100.
- 497 [8] Guyomar D, Aurelle N, Richard C, Gonnard P, Eyraud L. Non linearities in Langevin  
498 transducers. *Proc IEEE Ultrason Symp* 1994;**1051**:925-928.
- 499 [9] Guyomar D, Ducharme B, Sebald G. High nonlinearities in Langevin transducer: A  
500 comprehensive model. *Ultrasonics* 2011;**51**:1006-1013.
- 501 [10] Mathieson A, Cardoni A, Cerisola N, Lucas M. The influence of piezoceramic stack  
502 location on nonlinear behavior of Langevin transducers. *IEEE Ultrason Ferroelec Freq*  
503 *Contr Soc* 2013;**60**:1126-1133.
- 504 [11] Birkin PR, Leighton TG, Power JF, Simpson MD, A. Vinçotte ML, Joseph PF.  
505 Experimental and theoretical characterization of sonochemical cells. Part 1. Cylindrical  
506 reactors and their use to calculate the speed of sound in aqueous solutions. *J Phys Chem*  
507 *A* 2003;**107**:306-320.
- 508 [12] Mitragotri S, Farrell J, Tang H, Terahara T, Kost J, Langer R. Determination of  
509 threshold energy dose for ultrasound-induced transdermal drug transport. *J Contr Rel*  
510 2000; 63:41-52.
- 511 [13] Mitragotri S, Edwards DA, Blankschtein D, Langer R. A mechanistic study of  
512 ultrasonically-enhanced transdermal drug delivery. *J Pharm Sci* 1995;**84**:697-706.

- 513 [14] Emi T, Michaud K, Orton E, Santilli G, Linh G, O'Connell M, Issa F, Kennedy S.  
514 Ultrasonic generation of pulsatile and sequential therapeutic delivery profiles from  
515 calcium-crosslinked alginate hydrogels. *Molecules* 2019;**24**:1048.
- 516 [15] Gerayeli F. Stimulated delivery of therapeutic molecules from hydrogels using  
517 ultrasound. *PhD Thesis. Université Grenoble Alpes* 2017;NNT-2017GREAS019.
- 518 [16] Zamora-Moraa V, Velascob D, Hernández R, Mijangosa C, Kumachevaa E.  
519 Chitosan/agarose hydrogels: Cooperative properties and microfluidic preparation.  
520 *Carbohydr Polym* 2014;**111**:348-355.
- 521 [17] Fujiyabe T, Li X, Chung U, Sakai T. Diffusion behavior of water molecules in  
522 hydrogels with controlled network structure. *Macromolecules* 2019;**52**:1923-1929.
- 523 [18] Axpe E, Chan D, Offeddu GS, Chang Y, Merida D, Hernandez HL, Appel EA. A  
524 multiscale model for solute diffusion in hydrogels. *Macromolecules* 2019;**52**:6889-  
525 6897.
- 526 [19] Holmes DL, Stellwagen NC. The electric field dependence of DNA mobilities in  
527 agarose gels: a reinvestigation. *Electrophoresis* 1990;**11**:1-5.
- 528 [20] Dillon GP, Yu X, Sridharan A, Ranieri JP, Bellamkonda RV. The influence of physical  
529 structure and charge on neurite extension in a 3D hydrogel scaffold. *J Biomater Sci*  
530 *Polym Ed* 1998;**9**:1049-1069.
- 531 [21] Juntanon K, Niamlang S, Rujiravanit R, Sirivat A. Electrically controlled release of  
532 sulfosalicylic acid from crosslinked poly(vinyl alcohol) hydrogel. *Int J Pharmaceutics*  
533 2009;**356**:1-11.
- 534 [22] Singh TRR, Woolfson AD, Donnelly RF. Investigation of solute permeation across  
535 hydrogels composed of poly(methyl vinyl ether-co-maleic acid) and poly(ethylene  
536 glycol). *J Pharm Pharmacol* 2010;**62**:829-837.

- 537 [23] Marras-Marquesz T, Pena J, Veiga-Ochoa MD. Agarose drug delivery systems  
538 upgraded by surfactants inclusion: Critical role of the pore architecture. *Carbohydr*  
539 *Polym* 2014;**103**:359-368.
- 540 [24] Nugent MJD, Higginbotham CL. Preparation of a novel freeze thawed poly(vinyl  
541 alcohol) composite hydrogel for drug delivery applications. *Europ J Pharm Biopharm*  
542 2007;**67**:377-386.
- 543 [25] Hänggi P, Marchesoni F. Artificial Brownian motors: Controlling transport on the  
544 nanoscale. *Rev Modern Phys* 2009;**81**:387-442.
- 545 [26] Martin DK. Low-frequency ultrasound can drive the transport of nanoparticles.  
546 *EuroBiotech J* 2019;**3**:1-9.
- 547 [27] Lavon I, Kost J. Mass transport enhancement by ultrasound in non-degradable  
548 polymeric controlled release systems. *J Contr Rel* 1998;**54**:1-7.
- 549 [28] Aschkenasy C, Kost J. On-demand release by ultrasound from osmotically swollen  
550 hydrophobic matrices. *J Contr Rel* 2005;**110**:58-66.
- 551 [29] Manaspon C, Hernandez C, Nittayacharn P, Jeganathan S, Nasongkla N, Exner AA.  
552 Increasing distribution of drugs released from in situ forming PLGA implants using  
553 therapeutic ultrasound. *Annal Biomed Eng* 2017;**45**:28792887.
- 554 [30] Jiang H, Tovar-Carrillo K, Kobayashi T. Ultrasound stimulated release of mimosa  
555 medicine from cellulose hydrogel matrix. *Ultrason Sonochem* 2016;**32**:398-406.
- 556 [31] Boucaud A, Garrigue MA, Machet L, Vaillant L, Patat FJ. Effect of sonication  
557 parameters on transdermal delivery of insulin to hairless rats. *J Contr Rel* 2002;**81**:113-  
558 119.
- 559 [32] Sindeeva OA, Gusliakova OI, Inozemtseva OA, Abdurashitov AS, Brodovskaya EP,  
560 Gai M, et al. Effect of a controlled release of epinephrine hydrochloride from PLGA  
561 microchamber array: in vivo studies. *ACS Appl Mater Interfaces* 2018;**10**:37855-37864.

Figure 1



Size	$h_1$ (mm)	$h_2$ (mm)	$d_1$ (mm)	$d_2$ (mm)
Small	15	0	3	3
Medium	10	1	9	3
Large	10	2	14	4

Figure 2

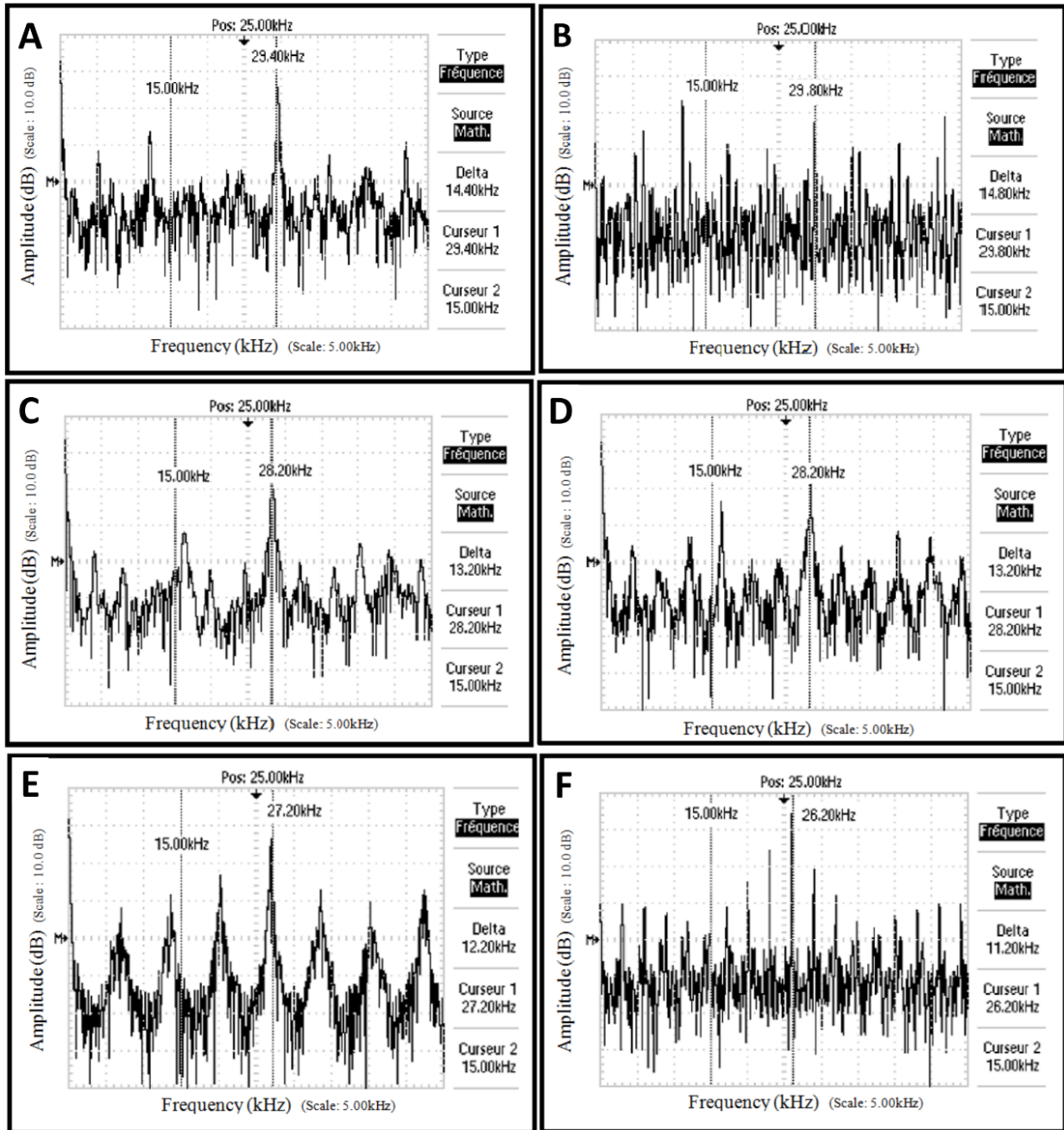


Figure 3

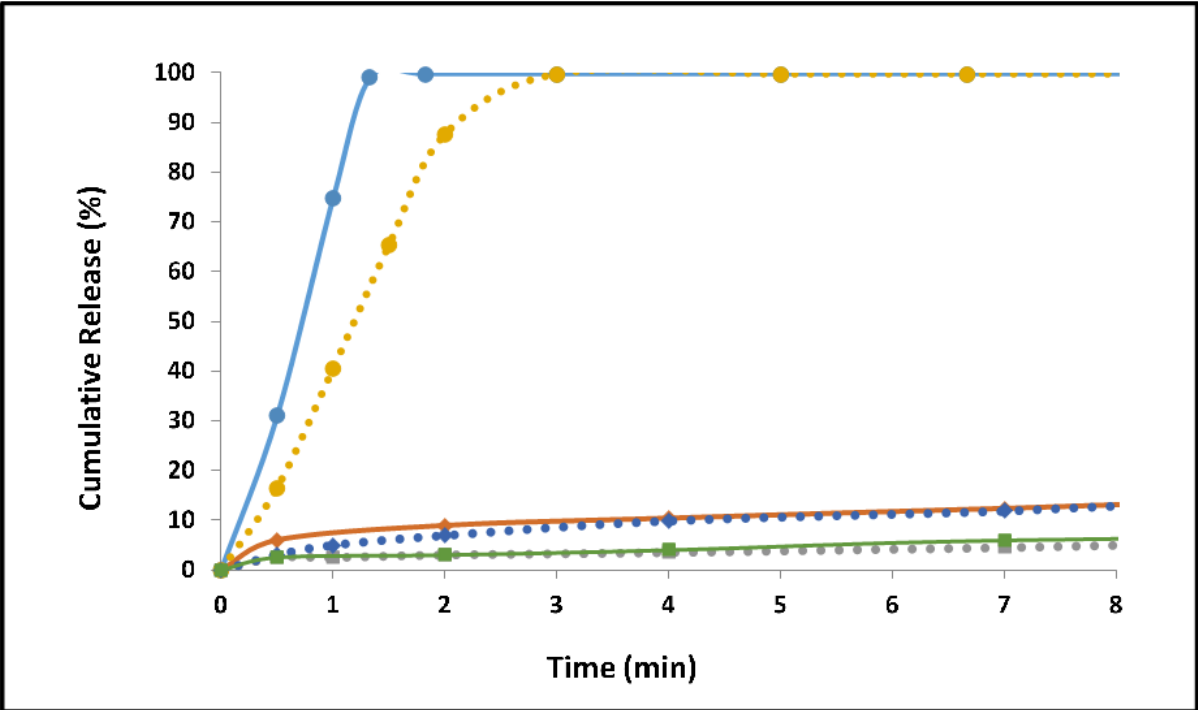


Figure 4

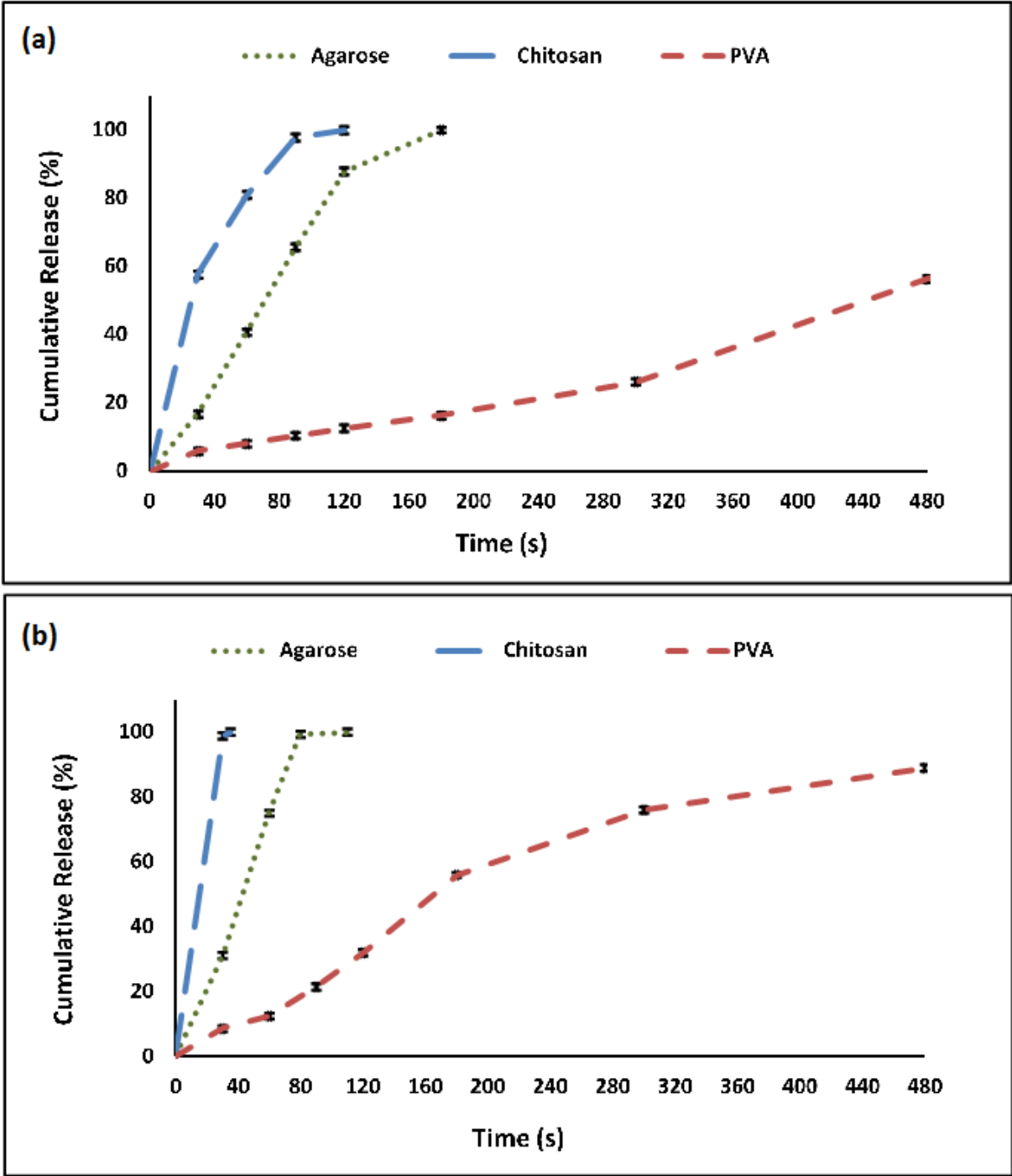
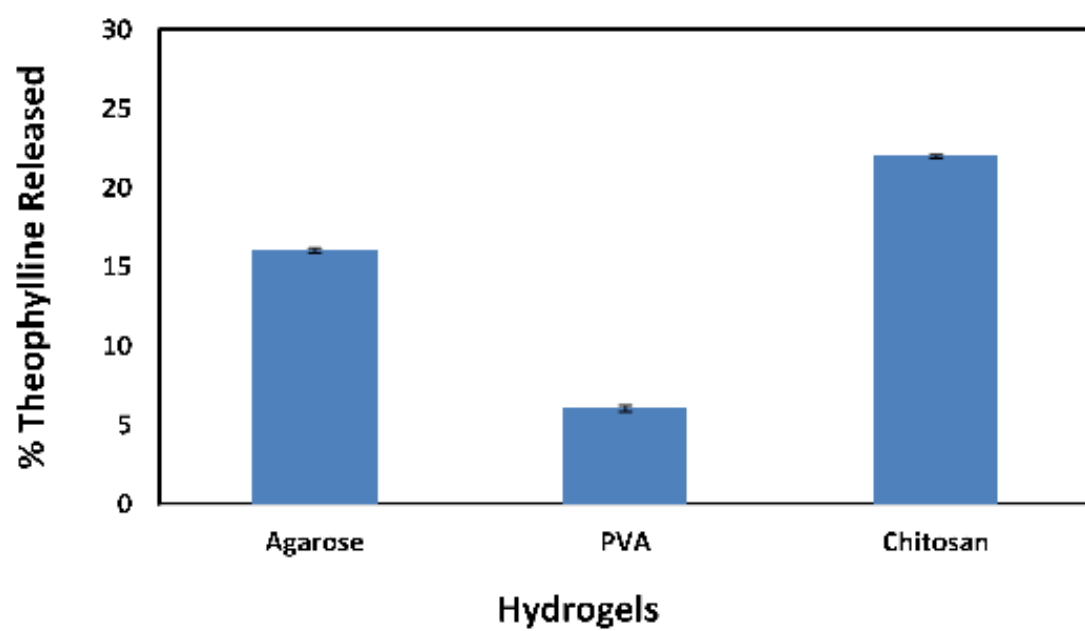


Figure 5



Graphical Abstract

